SUPPLEMENTARY FIGURE LEGENDS

Supplementary Figure 1. Analysis of in vivo phosphorylation of C-terminal WRN fragment

Analysis HEK293T cells were transfected with an expression construct encoding an N-terminal-truncated form of WRN protein (Myc-WRNΔN; for details see "Supplementary Materials and Methods) and treated with 10μM CPT for 6h. Cell lysates were subjected to Phos-tag SDS-PAGE followed by Western immunoblotting with an anti-Myc tag antibody. Where indicated, cell lysates were treated with 400 units of λ-phosphatase (λPPase). α, β and γ designate the different phosphorylated forms of Myc-WRNΔN protein. PCNA was used as loading control.

Supplementary Figure 2. Analysis of WRN and γ-H2AX colocalisation after HU treatment

WS*WRN* and WSWRN^{6A} cells were treated with HU for the indicated time and subjected to immunofluorescence using anti-WRN and anti-γ-H2AX antibodies. The graph shows the percentage of WRN-positive nuclei that colocalise with γ-H2AX. The data are means from triplicate experiments. A representative image from WSWRN^{6A} cells treated with HU for 8h is presented. Scale bars: 10μm.

Supplementary Figure 3. Analysis of integrity of the S/M checkpoint after HU treatment

WS*WRN*, WS and WSWRN^{6A} cells were transfected with control siRNAs (siCtrl) or siRNAs directed against ATR (siATR) and 48h later treated with 2mM HU for the indicated time, prior to analysis of S/M transition by evaluation of mitotic cells. Mitotic index (MI) was determined using phospho-Histone H3 immunostaining and presented as percent of untreated cultures. Data are means of three independent experiments. Error bars represent standard errors.

Supplementary Figure 4. Analysis of RAD51 relocalisation in foci following etoposide-induced DSBs

WS, WS*WRN* or WSWRN^{6A} cells were treated with 10μM etoposide (Etop) for the indicated times, prior to the analysis of RAD51 relocalisation in foci by immunofluorescence. Images shown derive from cells treated with etoposide for 6h. Graph shows the percentage of RAD51-positive nuclei for each experimental point. Data are presented as mean ± SE from three independent experiments. Scale bars: 10μm.

Supplementary Figure 5. Analysis of DSB accumulation in WS$WRN^{ATMdead}$ cells

(A) WB analysis of WRN protein levels in WS*WRN* and WS$WRN^{ATMdead}$ cells. Tubulin was used as loading control. (**B**) WS*WRN*, WS$WRN^{ATMdead}$ and WSWRN^{6A} cells were treated with 2mM HU for the indicated times prior to be subjected to γ-H2AX immunostaining. Representative images are shown. Scale bars: 10μm. Graph shows the percentage of γ-H2AX-positive nuclei for each experimental condition. (**C**) Analysis of ATM activation in ATR depleted cells following recovery from HU-mediated replication arrest. WS*WRN* cells were transfected with control siRNAs (siCtrl) or siRNAs directed against ATR (siATR) and 48h later treated with 2mM HU for the indicated time, prior to being recovered for 3h. Lysate were separated by SDS-PAGE and ATM activation was evaluated after WB using an anti-pS1981-ATM antibody. Total ATM was used to normalise the level of ATM phosphorylated. Data are representative of three independent experiments.

Supplementary Figure 6. Analysis of RAD51 relocalisation in foci following treatment with CPT in the absence of ATM-dependent phosphorylation of WRN

(A) WS*WRN*, WS$WRN^{ATMdead}$ or WSWRN^{6A} cells were treated with 10μM CPT for 8h, with or without 4h recovery, and analysed for the RAD51 relocalisation in foci by immunofluorescence. When indicated cells were grown in the continuous presence of 10μM KU55933 (iATM). Images

shown derive from cells treated with CPT and recovered for 4h. Scale bars: 10μm. Graph shows the percentage of RAD51-positive nuclei for each experimental point. Data are presented as mean ± SE from three independent experiments. (**B**) WS*WRN* cells were transfected with control siRNAs (siCtrl) or siRNAs directed against ATR (siATR), 48h later treated with 10μM CPT for 8h followed by recovery in drug-free medium for 4h and analysed for the RAD51 relocalisation in foci by immunofluorescence. When indicated cells were grown in the continuous presence of 10μM KU55933 (iATM). Graph shows the percentage of RAD51-positive nuclei for each experimental point. Data are presented as mean ± SE from three independent experiments. Scale bars: 10μm.

SUPPLEMENTARY MATERIALS AND METHODS

Generation of the N-terminal deletion of WRN and analysis of mobility shift detection of phosphorylated protein

To generate the pCMV-Myc-WRNΔN construct, the WRN C-terminal fragment, spanning amino-acids 940-1432, was subcloned from the pGEX4T-1-CWRNwt vector into the pCMV-Myc vector (a gift of Dr. Filippo Rosselli, CNRS, Villejuif, France). The N-terminal truncated fragment of WRN (WRNΔN) contains the Myc epitope for detection and the NLS for proper subnuclear localisation and retains the ability to form nuclear foci in response to replication arrest. Mobility shift detection of Myc-WRNΔN was achieved by Phos-Tag SDS-PAGE as described in Kinoshita et al., (2006) using 50μM Phos-Tag and 100μM $MnCl_2$.

SUPPLEMENTARY REFERENCE

Kinoshita E, Kinoshita-Kikuta E, Takiyama K, and Koike T (2006) Phosphate-binding tag: A new tool to visualize phosphorylated proteins. *Molecular and Cellular Proteomics* **5**: 749-757

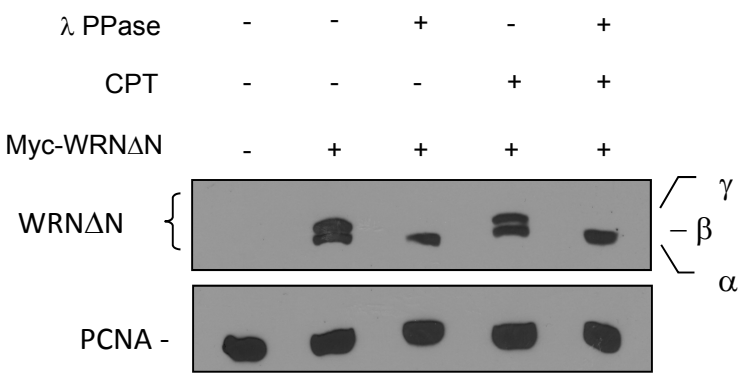

Supplementary Figure 1

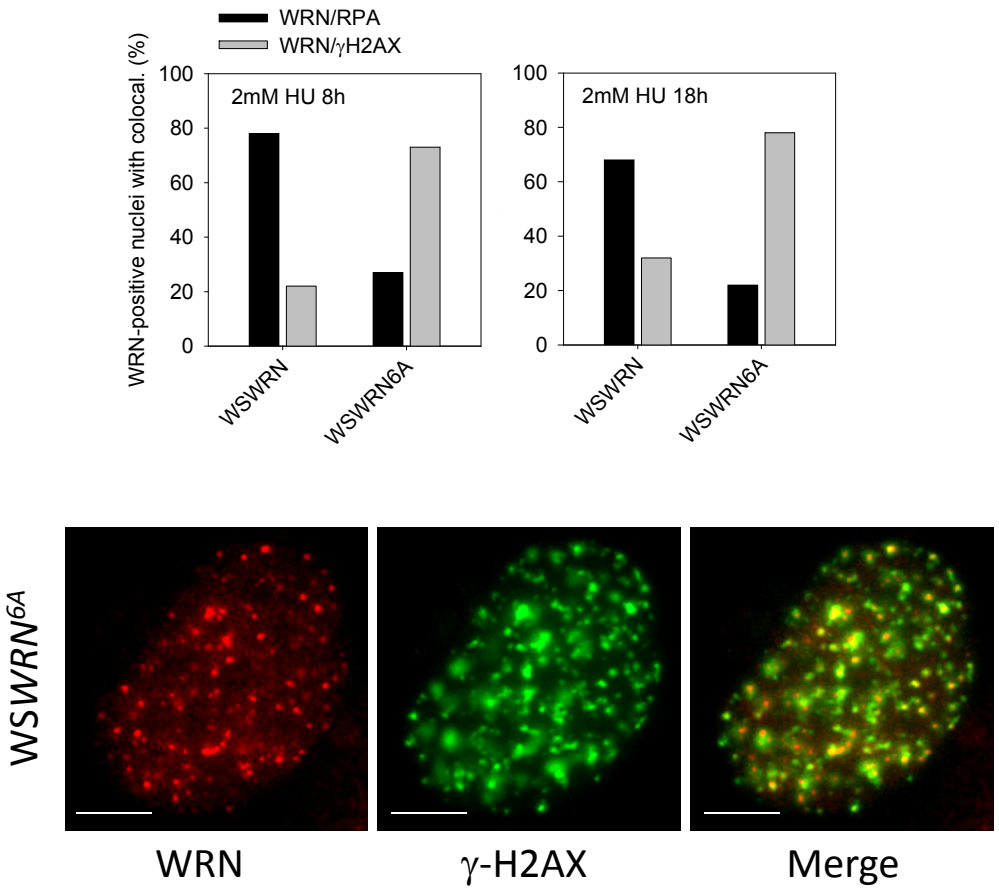

Supplementary Figure 2

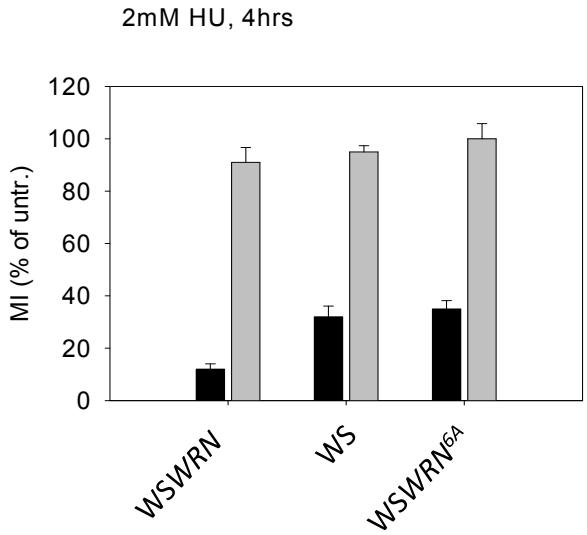

Supplementary Figure 3

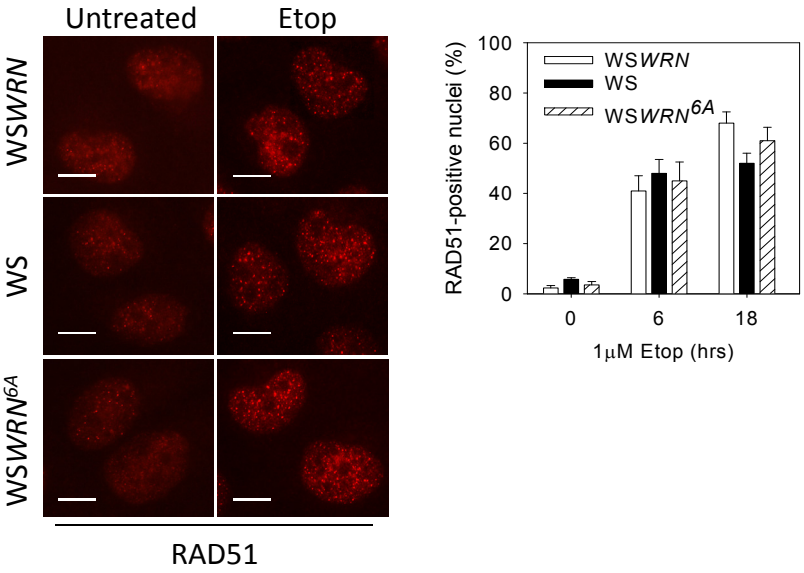

Supplementary Figure 4

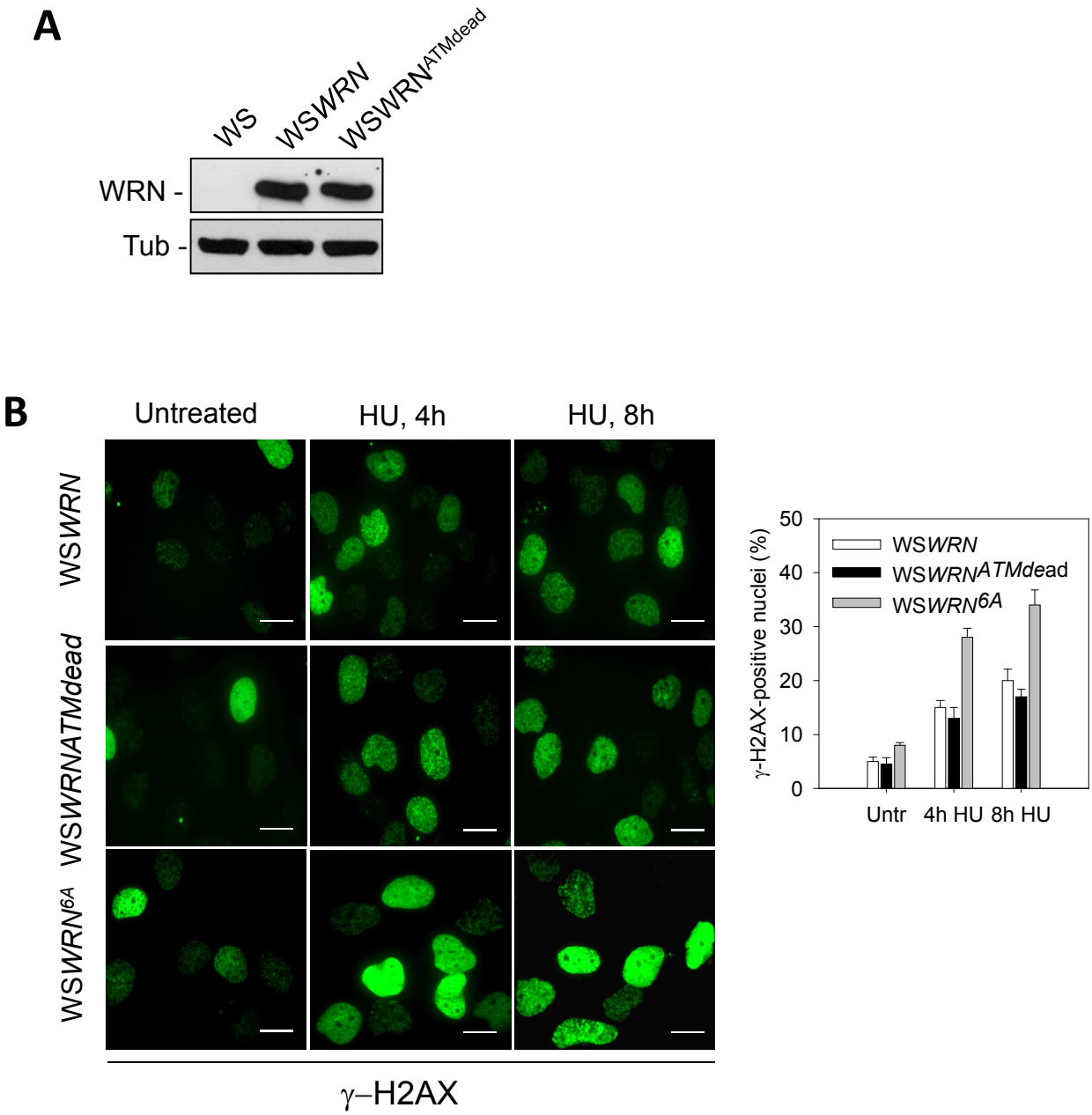

Supplementary Figure 5

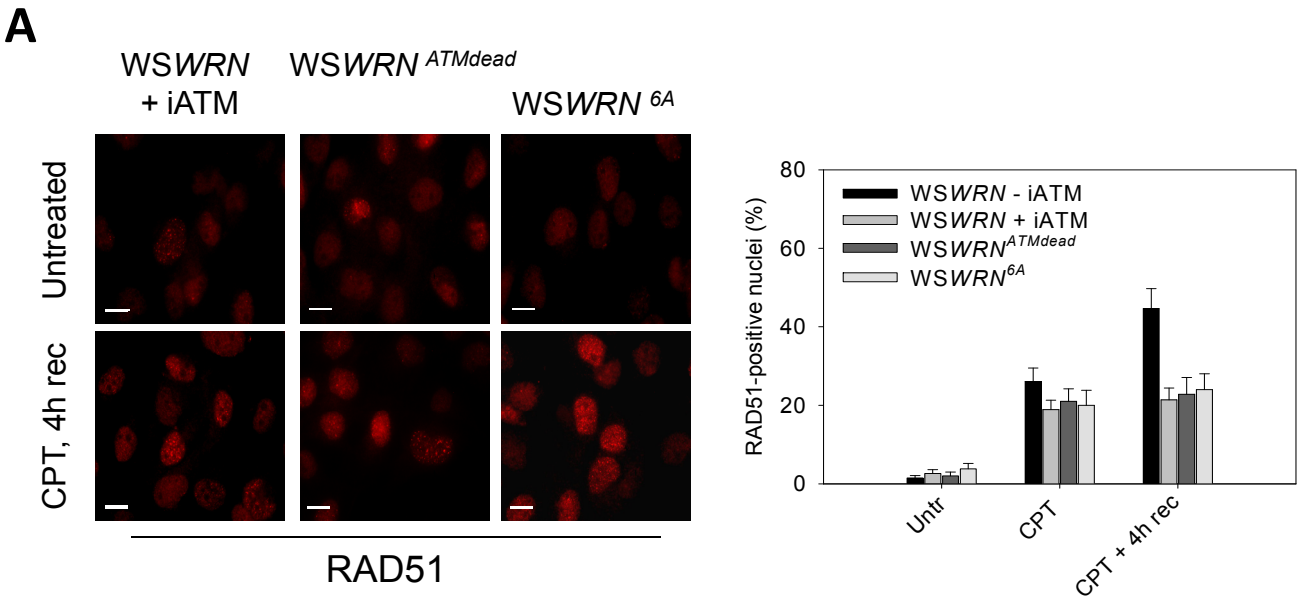

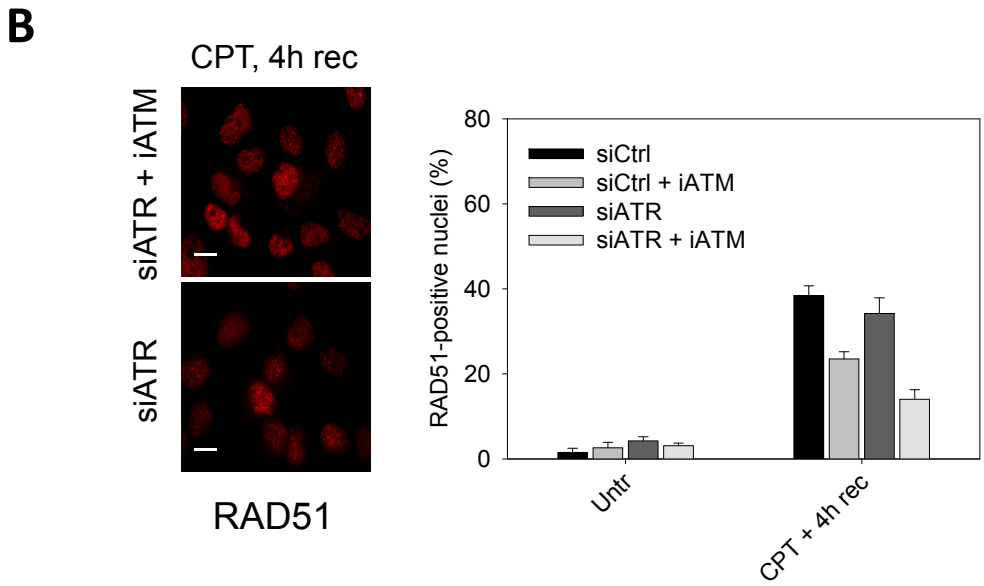

Supplementary Figure 6